Science & Technology Development Journal – Engineering and Technology, 4(4): 1313-1320

Open Access Full Text Article

Bài nghiên cứu

Electronic properties of defective graphene functionalized with oxygen and hydroxyl groups for molecular sieve

Vinh-Dat Vuong[1,2,3], Pham Tan Thi[1,2], Anh Quang Vu[1,2], Thang Van Le[1,2,*]

Use your smartphone to scan this QR code and download this article

ABSTRACT

Sub nanometer-defective-graphene, such as graphene with vacancies and graphene oxide, is promising candidates to overcome the water permeability of membrane materials for reverse osmosis technology, which is the leading technology for desalination and water treatment. The advantage of graphene-based materials in this area is attributed to their ability to adsorb contaminants by oxygen-containing functional groups at defects on graphene sheets. In this study, the interaction mechanism between water molecules and defective graphene, including pyridine defective graphene and pyridine graphene oxide, is described through electronic properties by a DFT calculation. The calculation was performed using the pseudopotential plane-wave method by Quantum Espresso with cut-off energy of 40 Rdy and supercell of 4x4 with in-plane periodicity containing 32 atoms. The orbital hybridization of C atom changed from sp^2 to sp^3 when it bonded to the O atom instead of neighboring C atoms in the graphene structure, led to the formation of a negative charge on the graphene sheet. In particular, hybrid sp^2/sp^3 orbitals was created on C atoms, which formed the epoxy group with the adsorption energy of -5.80 eV. In the models of monovacancy of graphene (defective graphene) and various positions of oxygen on defective graphene (graphene oxide), charge re-arrangement due to vacancy or presence of oxygen atom and weak binding energy between graphene and water molecules are responsible for attracting cations and allowing water molecules to pass through. The negative charge areas were thought to help increase the spacing of the functionalized defective graphene sheets, creating a path for water molecules to pass through. In addition, the computational model also showed the (non)-magnetic moment of the functionalized defective graphene depending on the functional group attached at the defect position.

Key words: desalination, water permeability, defective graphene, graphene oxide, DFT

[1]*Ho Chi Minh City University of Technology (HCMUT), 268 Ly Thuong Kiet, Ward 14, District 10, Ho Chi Minh City, Viet Nam*

[2]*Vietnam National University Ho Chi Minh City, Quarter 6, Linh Trung Ward, Thu Duc City, Vietnam*

[3]*Graduate University of Science and Technology, 18 Hoang Quoc Viet, Cau Giay, Hanoi City, Vietnam*

Correspondence

Thang Van Le, Ho Chi Minh City University of Technology (HCMUT), 268 Ly Thuong Kiet, Ward 14, District 10, Ho Chi Minh City, Viet Nam

Vietnam National University Ho Chi Minh City, Quarter 6, Linh Trung Ward, Thu Duc City, Vietnam

Email: vanthang@hcmut.edu.vn

History

- Received: 04-11-2021
- Accepted: 15-02-2022
- Published: 22-02-2022

DOI : 10.32508/stdjet.v4i4.932

Check for updates

INTRODUCTION

Two-dimensional graphene and its derivative materials such as graphene oxide, defective graphene, functionalized defective graphene have received a lot of interest both scientifically and technologically. These are promising materials for future technological fields including nanoelectronics, hydrogen storage, catalysis, composite devices, and chemical sensors [1–9]. Functionalized graphene with hydrogen, oxygen-containing groups, or other elements and chemical groups is of great interest as a way to engineer different properties [10,11].

Structural defects of graphene are caused by the synthesis on a large scale [12]. Defects change essentially not only the electronic properties but also the chemical properties of graphene. By functionalizing defects, it provides a way to modify the electronic and crystal structure of graphene, which may be important for practical applications such as graphene-based nanoelectronics and membranes [13,14]. Moreover, defective graphene functionalized with different functional groups varies the spacing between stacked sheets imparting highly selected molecular sieving membranes [15–17].

In this work, the electronic structure included graphene with monovacancy (denoted defective graphene hereafter) and its functionalization with oxygen and hydroxyl groups. The oxygen functionalized structure created a negative charge on the surface of the sheet which can prevent aggregation between sheets. More interestingly, defective graphene and defective graphene with oxygen and hydroxyl groups exhibited a finite magnetic moment.

METHODS

The calculations were based on the spin-polarized density functional theory (DFT) [18] using ab initio pseudopotential plane-wave method in the PWSCF code of the Quantum ESPRESSO distribution [19]. The generalized gradient approximations (GGA) for the exchange and correlation energies in the form were

Cite this article : Vuong V, Thi P T, Vu A Q, Le T V. **Electronic properties of defective graphene functionalized with oxygen and hydroxyl groups for molecular sieve**. *Sci. Tech. Dev. J. – Engineering and Technology;* 4(4): 1313-1320.

proposed by Perdew et al.[20] and the ultrasoft pseudopotentials from the Quantum ESPRESSO version 6.4.1 (2019)[21] were used. The valence electronic wave functions were expanded onto a plane-wave basis set with a kinetic energy cutoff of 40 Rdy for wave functions and 400 Rdy for charge density. Integration over the k-points has been carried out with smearing techniques[22] using a Gaussian broadening of 0.01 Rdy and a 3 x 3 x 1 Γ-centered Monkhorst-Pack k-point mesh[23]. Convergence tests with 7 x 7 x 1 k-point mesh have been carried out. Graphene sheets with vacancy or adsorbed molecules were simulated in hexagonal supercells with 4 x 4 in-plane periodicity containing 32 atoms.

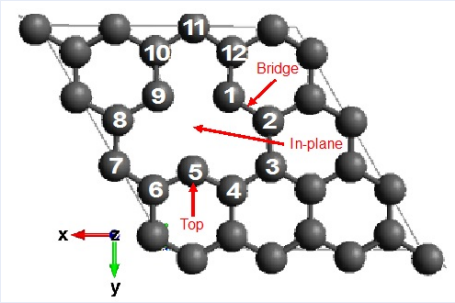

Figure 1: Model of defective graphene and sites of all carbon atoms surrounding defective site.

Defective graphene sheets were constructed by removing one single carbon atom and denoted positions of all carbon atoms around the defective site (Figure 1). The interacted energies of an oxygen atom and hydroxyl (OH) group with carbon atoms were calculated at the position given in Table 1. Formation and adsorption energies were determined by:

$$E_{Formation} = E_{Gr-Def} - E_{Gr(31-atoms)} - E_{Funct.} \quad (1)$$

$$E_{Ads.} = E_{Gr-Def+Funct.} + E_{Gr} - E_{Funct.} - E_{Gr-Def} \quad (2)$$

Where

- $E_{Formation}$ is the formation energy of the system
- E_{Gr-Def} is the energy of defective graphene
- $E_{Gr(31-atoms)}$ is the energy of graphene with 31 atoms
- $E_{Funct.}$ is the energy of functional groups (oxygen or hydroxyl)
- $E_{Ads.}$ is the adsorption energy of the system
- $E_{Gr-Def+Funct.}$ is the energy of defective graphene with the functional group
- E_{Gr} is the energy of pristine graphene

RESULTS AND DISCUSSION

Pristine graphene and defective graphene

The calculations were verified through the density of state (DOS), the partial density of state (PDOS) for the relative contribution of carbon orbitals, and the lattice parameter of pristine graphene. The calculated lattice parameter of graphene was 2.47 Å, which was in well agreement with the experimental value of 2.45 Å. DOS of pristine graphene has no spin polarization and is semi-metallic with Dirac cone at the Fermi level, corresponding to $E = 0$ eV in the DOS. The contribution to DOS closed Fermi level was mainly due to the π-orbital of carbon. Such results were in agreement with some previous publications[24,25].

The defective graphene was constructed with monovacancy by removing one carbon atom on pristine graphene and performed geometry optimization (Figure 1). Due to the breaking bonds of C-C, carbon atoms around the defective position form dangling bond sp^2[26,27]. Furthermore, the distance between carbon atoms at the defective position was contracted for C_4-C_5, C_5-C_6, C_9-C_{10} and expanded for C_1-C_2, C_8-C_9.

The structural stability of defective graphene was evaluated by calculated formation energy. According to Eq. (1), formation energy was the energy difference of the system of 31 carbon atoms and one defect compared to the system of 32 carbon atoms. Such energy difference close to zero was said to be attributed to a stable structure. The calculated formation energy was 7.82 eV, which was in well agreement with experimental results[26,28,29]. A similar value was yielded from the larger supercell (8 x 8) of 127 carbon atoms. DOS of defective graphene had many differences compared to pristine graphene, especially at around the Fermi level. The DOS of Fermi level for a spin up and spin down at the Fermi were unequal, where spin-up has more DOS than spin down (Figure 2). The contribution to the DOS of the spin-up was from the π-orbital and the p_y of carbon atoms at the defective site. This DOS difference led to the interesting property of defective graphene's magnetism. The calculated magnetic moment was about 1.45 μB. This magnetism was generated from the breaking of the D_{3h} symmetry down to the C_{2v} symmetry of graphene induced by the Jahn-Teller strain[26,30].

Functionalized defective graphene with oxygen

From the constructed 31-carbon defective graphene model in Figure 1, an oxygen atom was placed in the

Table 1: Models of calculation for oxygen and hydroxyl at carbon atoms around the defective position on the graphene sheet.

Oxygen	Top(a)	C1	C2	C3	C4	C5
	Bridge(b)	C1-C2	C2-C3	C3-C4	C4-C5	
	In-plane(c)	C1-C5-C9				
Hydroxyl	Top(a)	C1	C2	C3	C4	C5
	In-plane(c)	C1-C5-C9				

(a) 'top' is denoted as top of each carbon atom
(b) 'bridge' is denoted connection between carbon atoms,
(c) 'in-plane' is at the defective site.

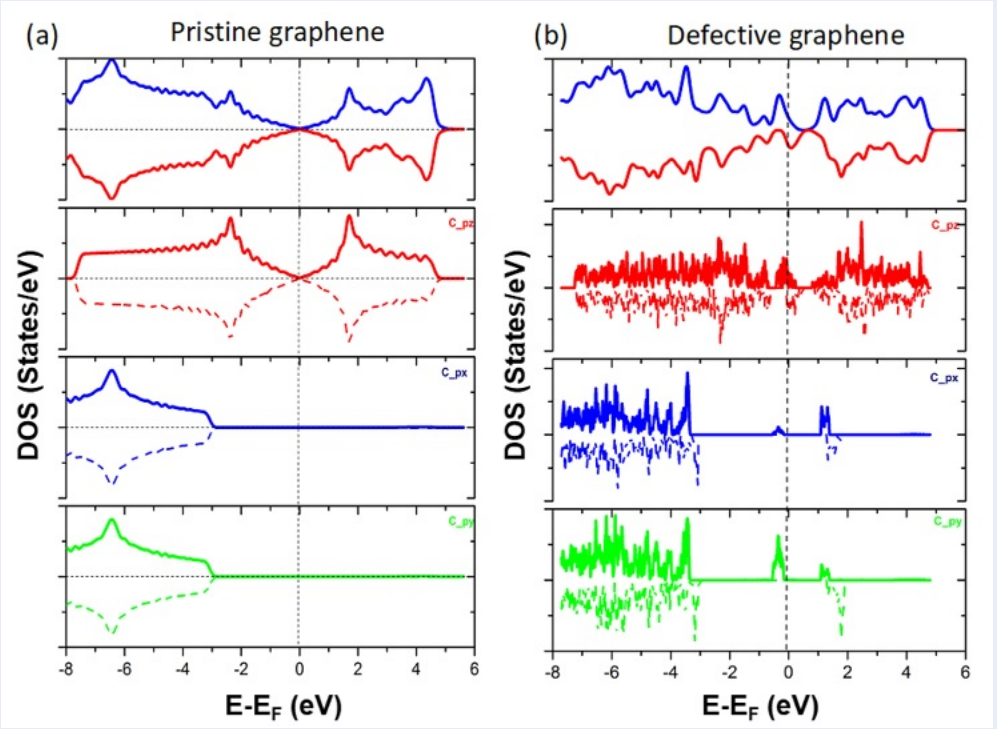

Figure 2: The density of state (DOS) of pristine graphene and defective graphene.

defect position. The oxygen adsorption sites and energy levels from the optimized structure were shown in Table 2. In the optimal structure, oxygen atom bonded to graphene sheet through two types of bonding: in-plane (Figure 3) and epoxy bridge (Figure 4). Calculated results showed that oxygen immediately replaced defective position (in-plane 159) with formation and adsorption energy of 0.40 eV and -5.80 eV, respectively. The oxygen at bridge 2-3 had similar formation and adsorption energy values to at in-plane 159. Such results confirmed the most formable and stable structures were in-plane and bridge, which were proposed previously[31]. The DOS of adsorption at the bridge cases was different from the in-plane case shown in Figure 4 andFigure 5. While the DOS of the in-plane 159 case showed a finite band-gap, the DOS around the Fermi level was contributed from the p_z orbital of the carbon and oxygen atoms (from PDOS below). The calculated magnetic moment gives zero value.

Adsorbed oxygen at bridge 2-3 has no bandgap (Figure 4). The PDOS graph showed that the p_z orbital of carbon and oxygen atoms changed and contributed to the finite state of DOS at the Fermi level. The total DOS of spin-up was different compared to spin down, resulting in a finite magnetic moment of 1.68 μB (Table 2). When the C-O bond formed on epoxidized graphene, the orbital hybridization of the car-

Table 2: The energy level and magnetic moment of oxygen adsorption side in the optimized structure of graphene.

Model	Position	EFormation, eV	EBinding, eV	Magnetic Moment, μ_B
Oxygen on top 1	In-plane 159	0.40	-5.80	0.25
Oxygen on top 2	Bridge 2-3	0.40	-5.80	0.00
Oxygen on top 3	Bridge 2-3	0.38	-0.27	1.68
Oxygen in-plane	In-plane 159	0.40	-5.80	0.00
Oxygen on bridge 1-2	Bridge 1-2	3.98	-1.48	0.08
Oxygen on bridge 2-3	Bridge 2-3	5.90	0.44	1.28
Oxygen on bridge 3-4	Bridge 3-4	6.04	0.68	2.52
Oxygen on bridge 4-5	Bridge 4-5	4.00	-1.49	0.08

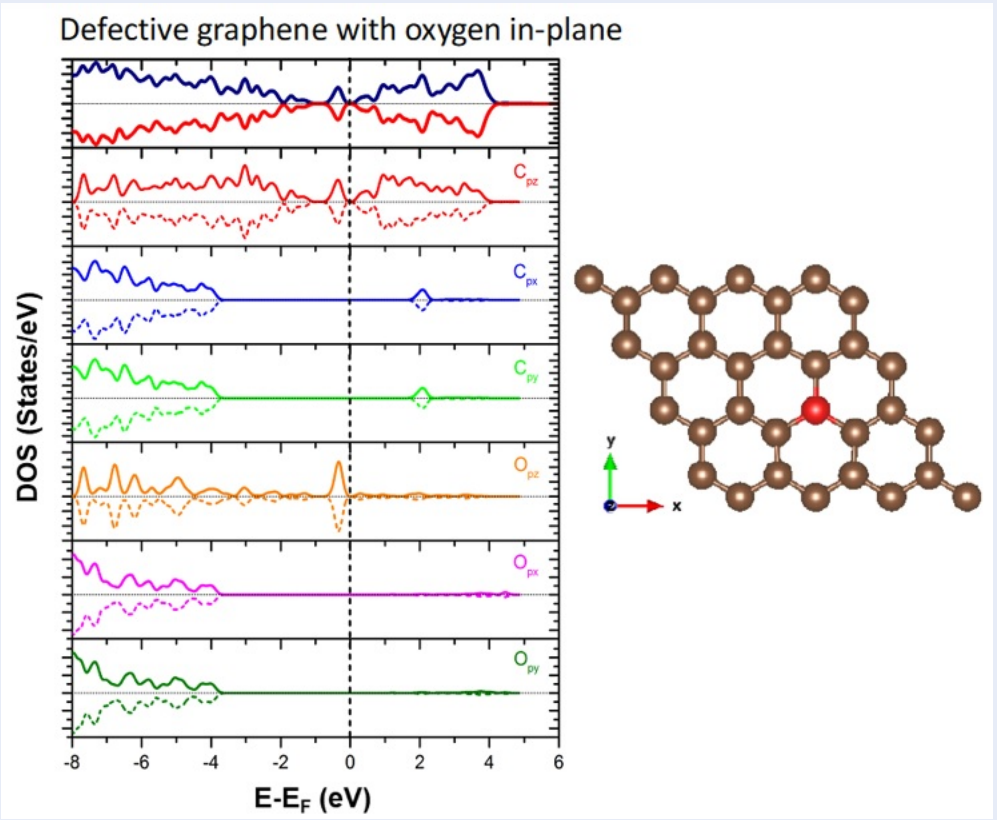

Figure 3: DOS of defective graphene with oxygen in-plane; illustration of the optimal structure.

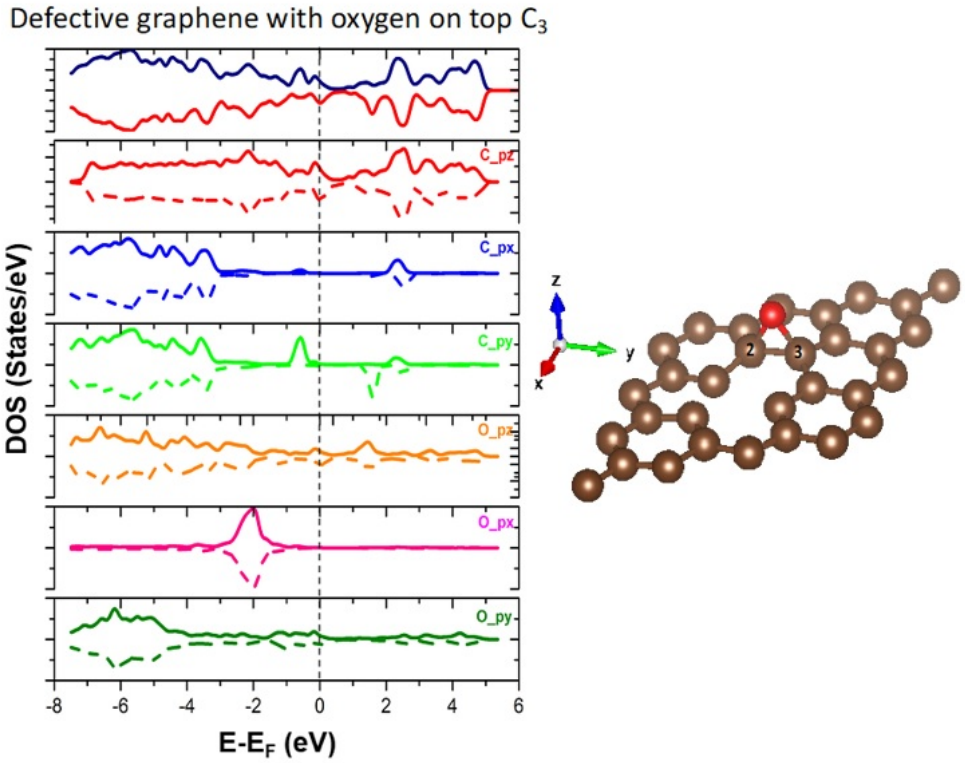

Figure 4: DOS of defective graphene with oxygen on top C_3; illustration of the optimal structure.

bon atom changed from sp^2 to sp^3 [32]. Functionalized graphene with oxygen-containing groups will generate a negative charge on the graphene sheet to prevent aggregation. This result was valuable filtration applications, where functionalized graphene with different groups can create a different type of voids towards a specific application. Another study demonstrated that hybrid sp^2/sp^3 orbitals produce nonlinear optical materials [33,34].

Functionalized defective graphene with a hydroxyl group

Figure 5 showed the calculated structures of hydroxyl defected, including the one-sided OH group with only oxygen atom bonded to two undercoordinated carbon atoms (Figure 5b) and dissociated OH group with oxygen and hydrogen atoms bonded to separated uncoordinated carbon atoms (Figure 5c). Dissociated process of hydroxyl had two steps: (i) breaking of the O-H bonding, which allows hydrogen atom to form C-H with undercoordinated carbon while oxygen atom forms a carbonyl group; (ii) forming the bonding between oxygen atom with two undercoordinated carbon atoms for an ether (C-O-C) group. This configuration has a total magnetization of 1.45 μ_B, mainly attributed to an unpaired π electron.

CONCLUSIONS

Density functional study showed its superiority for computing the electronic properties of pristine graphene, defective graphene, and functionalized defective graphene with oxygen and hydroxyl groups. Depending on the adsorption sites of oxygen, hydroxyl groups, the materials exhibit (non)-magnetic moment. Epoxy defective graphene created hybrid sp^2/sp^3 orbitals of carbon atoms and form a negative charge on the surface which prevents aggregation between graphene sheets. These results were important in the design of graphene-based molecular sieve membranes.

ACKNOWLEDGEMENTS

This research is funded by Vietnam National University Ho Chi Minh City (VNU-HCM) under grant number C2021-20-30. We acknowledge the support of time and facilities from Ho Chi Minh City University of Technology (HCMUT), VNU-HCM for this study.

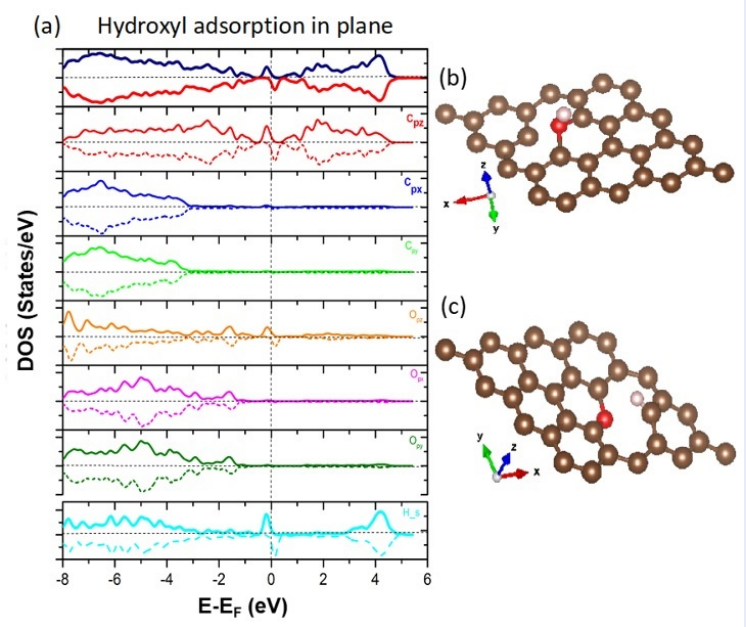

Figure 5: (a) DOS of defective graphene with hydroxyl group in-plane C_1-C_5-C_9. (b), (c) illustration of adsorption hydroxyl on top and in-plane C_1-C_5-C_9 on defective graphene.

COMPETING INTERESTS

The authors declare that they have no competing interests.

AUTHOR'S CONTRIBUTION

Conceptualization: Pham Tan Thi; Visualization: Thang Van Le; Methodology: Vinh-Dat Vuong, Anh Quang Vu; Data curation: Vinh-Dat Vuong; Validation: Anh Quang Vu, Pham Tan Thi; Software: Vinh-Dat Vuong, Pham Tan Thi; Writing – original draft: Vinh-Dat Vuong, Anh Quang Vu; Writing – review & editing: Pham Tan Thi, Thang Van Le.

REFERENCES

1. Fowler JD, et al. Practical Chemical Sensors from Chemically Derived Graphene. ACS Nano. 2009; 3(2):301-6;PMID: 19236064. Available from: https://doi.org/10.1021/nn800593m.
2. Gilje S, Han S, Wang M, Wang KL and Kaner RB. A Chemical Route to Graphene for Device Applications. Nano Lett. 2007; 7(11):3394-8;PMID: 17944523. Available from: https://doi.org/10.1021/nl0717715.
3. Geim AK and Novoselov KS. The rise of Graphene. Nat. Mater. 2007; 6:183-91;PMID: 17330084. Available from: https://doi.org/10.1038/nmat1849.
4. Wang Y, Liu J, Liu L and Sun DD. High-Quality Reduced Graphene Oxide-Nanocrystalline Platinum Hybrid Materials Prepared by Simultaneous Co-Reduction of Graphene Oxide and Chloroplatinic Acid. Nanoscale Res. Lett. 2011; 6(1):241;PMID: 21711745. Available from: https://doi.org/10.1186/1556-276X-6-241.
5. Yoo EJ, et al. Enhanced Electrocatalytic Activity of Pt Subnanoclusters on Graphene Nanosheet Surface. Nano Lett. 2009; 9(6):2255-9;PMID: 19405511. Available from: https://doi.org/10.1021/nl900397t.
6. Schedin F, Geim AK, Morozov SV, Hill EW, Blake P, Katsnelson MI, Novoselov KS. Detection of Individual Gas Molecules Adsorbed on Graphene. Nat. Mater. 2007; 6(9):652-5;PMID: 17660825. Available from: https://doi.org/10.1038/nmat1967.
7. Stankovich S, Dikin DA, Dommett GHB, et al. Graphene based Composite Materials. Nature. 2006; 442(7100):282-6;PMID: 16855586. Available from: https://doi.org/10.1038/nature04969.
8. Eda G and Chhowalla M. Graphene-based Composite Thin Films for Electronics. Nano Lett. 2009; 9(2):814-8;PMID: 19173637. Available from: https://doi.org/10.1021/nl8035367.
9. Ramanathan T, Abdala AA, et al. Functionalized Graphene Sheets for Polymer Nanocomposites. Nat. Nanotechnol. 2008; 3(6):327-31;PMID: 18654541. Available from: https://doi.org/10.1038/nnano.2008.96.
10. Sofo JO. Graphene: A Two-Dimensional Hydrocarbon. Phys. Rev. B 2007; 75:153401;Available from: https://doi.org/10.1103/PhysRevB.75.153401.

11. Elias DC, et al. Control of Graphene's Properties by Reversible Hydrogenation: Evidence for Graphane, Science. 2009; 323(5914):610-3;PMID: 19179524. Available from: https://doi.org/10.1126/science.1167130.
12. Skoda M, Dudek I, Jarosz A and Szukiewicz D. Graphene: One Material, Many Possibilities - Application Difficulties in Biological Systems. Journal of Nanomaterials 2014; 2014:890246;Available from: https://doi.org/10.1155/2014/890246.
13. Abraham J, et al. Tunable Sieving of Ions Using Graphene Oxide Membranes. Nature Nanotech. 2017; 12:546-50;PMID: 28369049. Available from: https://doi.org/10.1038/nnano.2017.21.
14. You Y, et al. Graphene and Graphene Oxide for Desalination. Nanoscale 2016; 8:117-9;PMID: 26615882. Available from: https://doi.org/10.1039/C5NR06154G.
15. Elimelech M and Phillip WA. The Future of Seawater Desalination: Energy, Technology, and The Environment. Science 2011; 333:712-7;PMID: 21817042. Available from: https://doi.org/10.1126/science.1200488.
16. Han Y, Xu Z, Gao C. Ultrathin Graphene Nanofiltration Membrane for Water Purification. Adv. Funct. Mater. 2013; 23(29):3693-700;Available from: https://doi.org/10.1002/adfm.201202601.
17. Liu GP, et al. Graphene-based Membranes. Chem. Soc. Rev. 2015; 44:5016-30;PMID: 25980986. Available from: https://doi.org/10.1039/C4CS00423J.
18. Jones RO, Gunnarxson O. The Density Functional Formalism, Its Applications and Prospects. Rev. Mod. Phys. 1989; 61:689;Available from: https://doi.org/10.1103/RevModPhys.61.689.
19. Giannozzi P, et al. QUANTUM ESPRESSO: A Modular and Open-Source Software Project for Quantum Simulations of Materials, J. Phys.: Condens. Matter. 2009; 21(39):395502;PMID: 21832390. Available from: https://doi.org/10.1088/0953-8984/21/39/395502.
20. Perdew JP, et al. Ernzerhof M. Generalized Gradient Approximation Made Simple, Phys. Rev. Lett. 1996; 77:3865;PMID: 10062328. Available from: https://doi.org/10.1103/PhysRevLett.77.3865.
21. We use C.pbe-rrkjus.UPF, O.pbe-rrkjus.UPF, H 1.007 H.pbe-rrkjus. UPF from the pseudopotential repository of;Available from: http://www.quantum-espresso.org.
22. Marzari N, Vanderbilt D, Payne MC. Ensemble Density-Functional Theory for Ab initio Molecular Dynamics of Metals and Finite-Temperature Insulators. Phys. Rev. Lett. 1997; 79:1337;Available from: https://doi.org/10.1103/PhysRevLett.79.1337.
23. Monkhorst HJ, Pack JD. Special Points for Brillouin-zone Integrations, Phys. Rev. B 1976; 13:5188;Available from: https://doi.org/10.1103/PhysRevB.13.5188.
24. Zheng J, et al. Diffusion of Li+ Ion on Graphene: A DFT Study. Appl. Surf. Sci. 2011; 258:1651-5;Available from: https://doi.org/10.1016/j.apsusc.2011.09.007.
25. Majidi R and Karami A. Adsorption of Formaldehyde on Graphene and Graphyne. Phys. E 2014; 59:169-73;Available from: https://doi.org/10.1016/j.physe.2014.01.019.
26. Ma Y, et al. Magnetic Properties of Vacancies in Graphene and Single-walled Carbon Nanotubes. New J. Phys. 2004; 6:68;Available from: https://doi.org/10.1088/1367-2630/6/1/068.
27. Kaloni TP, et al. Oxidation of Monovacancies in Graphene by Oxygen Molecules. J. Mater. Chem. 2011; 21:18284-8;Available from: https://doi.org/10.1039/c1jm12299a.
28. Denis PA. Density Functional Investigation of Thioepoxidated and Thiolated Graphene. J. Phys. Chem. C 2009; 113:5612-9;Available from: https://doi.org/10.1021/jp808599w.
29. Sknowron ST, et al. Energetics of Atomic Scale Structural Changes in Graphene. Chem. Rev. Soc. 2015; 44:3143-76;PMID: 25811047. Available from: https://doi.org/10.1039/C4CS00499J.
30. Nanda BRK, et al. Electronic Structure of The Subsitutional Vacancy in Graphene: Density-Functional and Green's Function Studies. New J. Phys. 2012; 14:083004;Available from: https://doi.org/10.1088/1367-2630/14/8/083004.
31. Mehmood F, Pachter R, Lu W and Boeckl J. Adsorption and Diffusion of Oxygen on Single Layer Graphene with Topological Defects. J. Phys. Chem. C 2013; 117:10366;Available from: https://doi.org/10.1021/jp312159v.
32. Lee D, et al. Magnetism in Graphene Oxide Induced by Epoxy Groups. Appl. Phys. Lett. 2015; 106:172402;Available from: https://doi.org/10.1063/1.4919529.
33. Speranza G. The Role of Functionalization in the Application of Carbon Materials: An Overview. Journal of Carbon Research C 2019; 5:84;Available from: https://doi.org/10.3390/c5040084.
34. Wang S, et al. The Role of sp2/sp3 Hybrid Carbon Regulation in Nonlinear Optical Properties of Graphene Oxide Materials, RSC Adv. 2017; 7:53643-52;Available from: https://doi.org/10.1039/C7RA10505C.

Tạp chí Phát triển Khoa học và Công nghệ – Kĩ thuật và Công nghệ, 4(4):1313-1320

Open Access Full Text Article

Bài nghiên cứu

Tính chất điện của graphene khuyết tật được chức năng hóa với oxy và nhóm hydroxyl ứng dụng cho rây phân tử

Vương Vĩnh Đạt[1,2,3], Phạm Tấn Thi[1,2], Vũ Anh Quang[1,2], Lê Văn Thăng[1,2,*]

Use your smartphone to scan this QR code and download this article

TÓM TẮT

Thẩm thấu ngược – công nghệ hàng đầu trong lĩnh vực xử lý nước và khử mặn – đang mở ra phạm vi ứng dụng tiềm năng cho các loại vật liệu mang khuyết tật có kích thước dưới nanomet như graphen có khuyết tật lỗ trống và graphen oxit (GO). Trong lĩnh vực này, ưu điểm của nhóm vật liệu graphene và dẫn xuất từ graphene là khả năng hấp phụ các tạp chất hoặc ion trong nước nhờ vào các nhóm chức chứa oxy được hình thành tại vị trí khuyết tật trên bề mặt graphen. Trong nghiên cứu này, các dạng khuyết tật pyridine trên bề mặt graphen và GO được nghiên cứu bằng lý thuyết phiếm hàm mật độ (DFT) nhằm tính toán cơ chế tương tác giữa các phân tử nước với các dạng khuyết tật này. Mô hình tính toán được thiết lập từ công cụ Quantum Espresso với năng lượng cắt 40 Rdy và trên cơ sở một supercell 4x4 gồm 32 nguyên tử đồng phẳng. Các mô hình graphen đơn khuyết (monovacancy) và mô hình GO với nguyên tử O ở các vị trí khác nhau đều cho thấy sự tái phân bố điện tích do vị trí của khuyết tật hoặc hiện diện của nguyên tử O. Khi các nguyên tử C trên mặt phẳng thay đổi từ liên kết C-C sang C-O, dạng lai hóa orbitan thay đổi từ sp^2 thành sp^3 là nguyên nhân hình thành điện tích âm trên bề mặt graphene. Đặc biệt, dạng lai hóa hỗn hợp sp^2/sp^3 được hình thành tại nhóm epoxy với năng lượng hấp phụ -5.80 eV. Các vùng điện tích âm phân bố trên bề mặt graphen tạo ra lực hút với các cation. Đồng thời, liên kết yếu giữa graphen và các phân tử nước cho phép cho phép chúng dễ dàng đi qua các lỗ trống trên cấu trúc vật liệu. Các vùng điện tích âm giúp tăng khoảng cách giữa các tấm graphen khuyết tật được chức hóa, tạo thành đường dẫn cho các phân tử nước đi qua.Mô hình tính toán cũng cho thấy graphen khuyết tật được chức hóa có momen từ phụ thuộc vào nhóm chức gắn vào vị trí khuyết tật.

Từ khoá: khử mặn, thẩm thấu, graphen khuyết tật, graphen oxit, lý thuyết phiếm hàm mật độ (DFT)

[1]*Trường Đại học Bách khoa, 268 Lý Thường Kiệt, Phường 14, Quận 10, Thành phố Hồ Chí Minh, Việt Nam*

[2]*Đại học Quốc gia TP. Hồ Chí Minh, Khu phố 6, Phường Linh Trung, Quận Thủ Đức, Việt Nam*

[3]*Học viện Khoa học và Công nghệ, 18 Hoàng Quốc Việt, Cầu Giấy, Hà Nội, Việt Nam*

Liên hệ

Lê Văn Thăng, Trường Đại học Bách khoa, 268 Lý Thường Kiệt, Phường 14, Quận 10, Thành phố Hồ Chí Minh, Việt Nam

Đại học Quốc gia TP. Hồ Chí Minh, Khu phố 6, Phường Linh Trung, Quận Thủ Đức, Việt Nam

Email: vanthang@hcmut.edu.vn

Lịch sử

- Ngày nhận: 04-11-2021
- Ngày chấp nhận: 15-02-2022
- Ngày đăng: 22-02-2022

DOI : 10.32508/stdjet.v4i4.932

Check for updates

Trích dẫn bài báo này: Đạt V V, Thi P T, Quang V A, Thăng L V. **Tính chất điện của graphene khuyết tật được chức năng hóa với oxy và nhóm hydroxyl ứng dụng cho rây phân tử**. *Sci. Tech. Dev. J. - Eng. Tech.;* 4(4):1313-1320